JHEP HYPER VERSION

Received: *July 26, 1999,* Accepted: *July 27, 1999*

Corrections of $\mathcal{O}(\alpha_S^2)$ to the forward-backward asymmetry*

Stefano Catani†

Theory Division, CERN CH-1211 Geneva 23, Switzerland
E-mail: stefano.catani@cern.ch

Michael H. Seymour

Rutherford Appleton Laboratory, Chilton Didcot,
Oxfordshire, OX11 0QX, England
E-mail: mike.seymour@rl.ac.uk

Abstract: We calculate the second-order QCD corrections to the forward-backward asymmetry in e^+e^- annihilation. Using the quark axis definition, we do not agree with either existing calculation, but the difference relative to one of them is small and understood. In particular, we point out that the forward-backward asymmetry of massive quarks is enhanced by logarithms of the quark mass. This implies that the forward-backward asymmetry of massless quarks is not computable in QCD perturbation theory and affected by non-power-suppressed corrections coming from the non-perturbative fragmentation functions. We also calculate the second-order corrections using the experimentally-preferred thrust axis definition for the first time.

Keywords: QCD, NLO Computations.

*This work was supported in part by the EU Fourth Framework Programme "Training and Mobility of Researchers", Network "Quantum Chromodynamics and the Deep Structure of Elementary Particles", contract FMRX–CT98–0194 (DG 12–MIHT).

†On leave of absence from INFN, Sezione di Firenze, Florence, Italy.

JHEP07(1999)023

Contents

JHEP07(1999)023

1. Introduction

Some of the most precise determinations of the weak mixing angle $\sin^2\theta_{\text{eff}}$ come from measurements of asymmetries in fermion production on the Z peak [1]. In particular, the forward-backward asymmetry of b quarks is measured with a precision of about 2%, allowing an extraction of $\sin^2\theta_{\text{eff}}$ with almost per mille accuracy. However, since we are dealing with quarks in the final state, we must ensure that QCD corrections, both perturbative and non-perturbative, are understood to at least the same precision. From simple power counting, it is clear that this necessitates including $\mathcal{O}(\alpha_S^2)$ perturbative and $1/Q$ non-perturbative effects. Even these will probably not be enough in the future, when linear e^+e^- colliders are hoped to reach a precision of order 0.1% [2].

The $\mathcal{O}(\alpha_S)$ perturbative corrections were first calculated in ref. [3] in the massless approximation. The mass corrections to this result were first calculated in ref. [4]

and were found to be significant $\sim \alpha_S m_b/M_Z$. These calculations used a slightly different definition of the asymmetry than the experimental measurements, which use the thrust axis rather than the quark direction. This difference was rectified in refs. [5, 6].

To date there have been two $\mathcal{O}(\alpha_S^2)$ calculations, both in the massless approximation using the quark direction. The classic calculation of Altarelli and Lampe [7] determined the $\mathcal{O}(\alpha_S^2)$ coefficient numerically and found it to be small. This result has been the basis of all the experimental analyses since. However, the recent analytical calculation by Ravindran and van Neerven [8] obtained a coefficient about four times bigger. This discrepancy is comparable to the size of the experimental errors and needs to be resolved before the final electroweak fits to the LEP1 data can be made. The $\mathcal{O}(\alpha_S^2)$-calculation using the experimentally-used thrust axis definition, would also be highly desirable.

In this paper we perform a numerical calculation of the $\mathcal{O}(\alpha_S^2)$ corrections to the forward-backward asymmetry, and compare our results with the existing calculations. We also calculate for the first time the corrections using the thrust axis definition rather than the quark direction.

The paper is set out as follows. In section 2 we define the forward-backward asymmetry and the closely-related left-right forward-backward asymmetry [9] and recall some features of the tree-level and $\mathcal{O}(\alpha_S)$ perturbative calculations. In section 3 we discuss the general set-up of the $\mathcal{O}(\alpha_S^2)$ calculation, and divide it into several parts. We pay particular attention to the four-b final state, which will turn out to play an important rôle in our calculation. In section 4 we make some final remarks on the details of the calculation, before presenting our results for the $\mathcal{O}(\alpha_S^2)$ coefficients with the two axis definitions. We also compare our results with the existing calculations. We discuss the impact of our results in section 5, and try to estimate the remaining theoretical errors. We leave some more technical details of the calculation to appendices A and B.

2. Definition and perturbative calculation

The simplest definition of the b-quark[1] forward-backward asymmetry A_{FB} is

$$A_{FB} = \frac{N_F - N_B}{N_F + N_B}, \tag{2.1}$$

where N_F and N_B are the number of b quarks observed in the forward and backward hemispheres, respectively.

[1] Throughout this paper we explicitly consider the case of the b-quark. The results for the charm quark can be simply obtained by properly replacing the mass and the electroweak couplings of the massive quark.

The axis that identifies the forward direction can be defined in a variety of ways. However, for the purpose of making $A_{\rm FB}$ computable in QCD perturbation theory, the axis must be defined in an infrared and collinear-safe manner. In this paper we explicitly consider two different definitions: the b-quark direction, and the thrust axis direction. The thrust axis has a two-fold ambiguity: we use the one that is nearer the b-quark direction. In the following, the forward-backward asymmetries with respect to the b-quark direction and to the thrust axis direction are denoted by $A_{\rm FB}^b$ and $A_{\rm FB}^T$, respectively.

According to the definition in eq. (2.1), $A_{\rm FB}$ can be expressed in an equivalent way in terms of the cross section

$$\frac{d\sigma(\mathrm{e}^+\mathrm{e}^- \to b + X)}{dx\, d\cos\theta}\,, \tag{2.2}$$

for inclusive b-quark production, where x is the fraction of the electron energy carried by the b quark and θ is the angle between the electron momentum and the direction defining the forward hemisphere (both energies and angles are defined in the centre-of-mass frame).

Starting from the distribution in eq. (2.2), we can introduce the forward and backward cross sections $\sigma_{\rm F}$ and $\sigma_{\rm B}$:

$$\sigma_F \equiv \int_0^1 d\cos\theta \int_0^1 dx \frac{d\sigma}{dx\, d\cos\theta}\,, \qquad \sigma_B \equiv \int_{-1}^0 d\cos\theta \int_0^1 dx \frac{d\sigma}{dx\, d\cos\theta}\,, \tag{2.3}$$

and the symmetric and antisymmetric cross sections $\sigma_{\rm S}$ and $\sigma_{\rm A}$:

$$\sigma_{\rm S} = \sigma_{\rm F} + \sigma_{\rm B}\,, \qquad \sigma_{\rm A} = \sigma_{\rm F} - \sigma_{\rm B}\,. \tag{2.4}$$

We can then write the forward-backward asymmetry as

$$A_{\rm FB} = \frac{\sigma_{\rm A}}{\sigma_{\rm S}}\,. \tag{2.5}$$

In the perturbative QCD calculation of $\sigma_{\rm S}$ and $\sigma_{\rm A}$, we have to evaluate the corresponding matrix element squared, which is given by the product $L_{\mu\nu}T^{\mu\nu}$ of the leptonic and hadronic tensors $L_{\mu\nu}$ and $T^{\mu\nu}$. Then we could perform the integration over the final-state parton momenta in $T^{\mu\nu}$ and finally the integration over the scattering angle θ. Nonetheless, it is more convenient to use a simplified procedure. We can indeed avoid having to explicitly integrate over the scattering angle, by first performing the angular integration of the leptonic tensor. Doing this, we can compute $\sigma_{\rm S}$ and $\sigma_{\rm A}$ by simply performing the integration over the final-state parton momenta of the following projections of the hadronic tensor:

$$\sigma_{\rm S} \propto -g_{\mu\nu}T^{\mu\nu}\,, \tag{2.6}$$

$$\sigma_{\rm A} \propto i\epsilon_{\mu\nu\lambda\rho}\frac{n^\lambda Q^\rho}{n\cdot Q}T^{\mu\nu}\,, \tag{2.7}$$

where Q^μ is the total incoming momentum and the light-like ($n^2 = 0$) vector n^μ identifies the forward direction.

2.1 Leading order

At the leading order (LO) we have to consider the cross sections for the process $e^+e^- \to b\bar{b}$ at the tree level and thus, the b-quark direction and the thrust direction coincide. The tree-level cross sections $\sigma_S^{(0)}$ and $\sigma_A^{(0)}$ are straightforward to calculate and the result is[2]

$$\sigma_S^{(0)} = \frac{4\pi\alpha^2 N_c}{3Q^2}\Bigg\{e_e^2 P_v e_b^2 + 2\frac{\big(Q^2 - M_Z^2\big)Q^2}{D_Z(Q^2)}\big(P_v e_e v_e + P_a e_e a_e\big)e_b v_b + \\ + \frac{Q^4}{D_Z(Q^2)}\Big[\big(v_e^2 + a_e^2\big)P_v + 2P_a v_e a_e\Big]\big(v_b^2 + a_b^2\big)\Bigg\}, \tag{2.8}$$

$$\sigma_A^{(0)} = \frac{4\pi\alpha^2 N_c}{3Q^2}\frac{3}{4}\Bigg\{2\frac{\big(Q^2 - M_Z^2\big)Q^2}{D_Z(Q^2)}\big(P_v e_e a_e + P_a e_e v_e\big)e_b a_b + \\ + \frac{Q^4}{D_Z(Q^2)}\Big[2P_v v_e a_e + P_a\big(v_e^2 + a_e^2\big)\Big]2v_b a_b\Bigg\}, \tag{2.9}$$

with

$$P_v = 1 + P_L P_R\,, \tag{2.10}$$

$$P_a = P_L + P_R\,, \tag{2.11}$$

where P_L is the left-hand-polarization of the electron ($+1$ = fully left-handed, 0 = unpolarized, -1 = fully right-handed) and P_R is the right-hand-polarization of the positron ($+1$ = fully right-handed and so forth),

$$D_Z\big(Q^2\big) = \big(Q^2 - M_Z^2\big)^2 + \big(\Gamma_Z M_Z\big)^2\,, \tag{2.12}$$

e_i is the electric charge in units of the proton charge (i.e., $e_e = -1$) and the electroweak couplings are:

$$v_i = \frac{1}{2\sin\theta_w\cos\theta_w}\big(t_{3i} - 2e_i\sin^2\theta_w\big)\,, \tag{2.13}$$

$$a_i = \frac{1}{2\sin\theta_w\cos\theta_w}t_{3i}\,. \tag{2.14}$$

The ratio between eqs. (2.8) and (2.9) is insensitive to the fine structure constant α and the number of colours N_c and thus, at LO the forward-backward asymmetry $A_{FB}^{(0)}$,

$$A_{FB}^{(0)} = \frac{\sigma_A^{(0)}}{\sigma_S^{(0)}} \tag{2.15}$$

[2]Unless explicitly mentioned, we neglect the b-quark mass throughout this paper. At LO the dominant mass corrections are proportional to m_b^2/Q^2 and can be found, for instance, in ref. [8].

gives a direct measurement of the electroweak couplings. In particular, if we are exactly on the resonance, $Q^2 = M_Z^2$, and we neglect the photon contribution, we obtain

$$A_{\rm FB}^{(0)} = \frac{3}{4}\frac{\mathcal{A}_e + \mathcal{P}}{1 + \mathcal{A}_e\mathcal{P}}\mathcal{A}_b\,, \tag{2.16}$$

where

$$\mathcal{A}_i = \frac{2v_i a_i}{v_i^2 + a_i^2}\,, \tag{2.17}$$

$$\mathcal{P} = \frac{P_a}{P_v} = \frac{P_{\rm L} + P_{\rm R}}{1 + P_{\rm L}P_{\rm R}}\,. \tag{2.18}$$

Finally, for unpolarized beams, we obtain

$$A_{\rm FB}^{(0)} = \frac{3}{4}\mathcal{A}_e\mathcal{A}_b\,. \tag{2.19}$$

This is the form in which the forward-backward asymmetry is most often presented. It is worth pointing out however that all of our results will be universal multiplicative corrections,[3] so apply equally well to any of the forms (2.15), (2.16) or (2.19).

Another important variable is the so-called left-right forward-backward asymmetry [9],

$$A_{\rm LR,FB} = \frac{N_{\rm F}(\mathcal{P}=+1) - N_{\rm F}(\mathcal{P}=-1) - N_{\rm B}(\mathcal{P}=+1) + N_{\rm B}(\mathcal{P}=-1)}{N_{\rm F}(\mathcal{P}=+1) + N_{\rm F}(\mathcal{P}=-1) + N_{\rm B}(\mathcal{P}=+1) + N_{\rm B}(\mathcal{P}=-1)}\,. \tag{2.20}$$

Its LO expression can be obtained from eqs. (2.8) and (2.9), and again neglecting the photon contribution exactly on the Z resonance, it is given by:

$$A_{\rm LR,FB}^{(0)} = \frac{3}{4}\mathcal{A}_b\,. \tag{2.21}$$

Our results apply equally well also to this observable.

2.2 Next-to-leading-order corrections

At next-to-leading order (NLO), we have to consider the one-loop cross sections $\sigma^{(1);\text{one-loop}}$ for the two-parton process $\mathrm{e^+e^-} \to b\bar{b}$ and the tree-level cross sections $\sigma^{(1);\text{tree}}$ for the three-parton process $\mathrm{e^+e^-} \to b\bar{b}g$. We obtain:

$$A_{\rm FB}^{(1)} = \frac{\sigma_{\rm A}^{(0)} + \sigma_{\rm A}^{(1);\text{one-loop}} + \sigma_{\rm A}^{(1);\text{tree}}}{\sigma_{\rm S}^{(0)} + \sigma_{\rm S}^{(1);\text{one-loop}} + \sigma_{\rm S}^{(1);\text{tree}}}\,. \tag{2.22}$$

Each of the cross sections at $\mathcal{O}(\alpha_{\rm S})$ is separately divergent, so they have to be regularized in some way before being combined together. In any regularization scheme

[3] At $\mathcal{O}(\alpha_{\rm S}^2)$ there are some non-universal corrections, but we do not explicitly compute them (see the discussion in sections 3.2 and 3.1).

that preserves the helicity conservation of massless QCD[4] (for example, dimensional regularization), we have the property

$$\frac{\sigma_{\rm A}^{(1);\text{one-loop}}}{\sigma_{\rm A}^{0}} = \frac{\sigma_{\rm S}^{(1);\text{one-loop}}}{\sigma_{\rm S}^{0}}\,, \tag{2.23}$$

and hence, if we expand the ratio in eq. (2.22) up to $\mathcal{O}(\alpha_{\rm S})$, the one-loop corrections cancel, and we obtain

$$A_{\rm FB}^{(1)} = \frac{\sigma_{\rm A}^{(0)}}{\sigma_{\rm S}^{(0)}}\left(1 + \frac{\sigma_{\rm A}^{(1);\text{tree}}}{\sigma_{\rm A}^{(0)}} - \frac{\sigma_{\rm S}^{(1);\text{tree}}}{\sigma_{\rm S}^{(0)}}\right). \tag{2.24}$$

Although $\sigma_{\rm A}^{(1);\text{tree}}$ and $\sigma_{\rm S}^{(1);\text{tree}}$ are each separately divergent in the soft and collinear regions, the divergences cancel at the integrand level, and the whole thing can be calculated in the unregularized theory.

At this order, the different definitions of the forward-backward asymmetry give different results. As already anticipated, we consider two possible definitions of the forward direction: the b-quark direction and the thrust axis direction.

It is straightforward to calculate the NLO corrections in eq. (2.24) analytically with either definition. We obtain:

$$A_{\rm FB}^{(1);b} = A_{\rm FB}^{(0)}\left(1 - \frac{3}{4}C_{\rm F}\frac{\alpha_{\rm S}}{\pi}\right) \simeq A_{\rm FB}^{(0)}\big(1 - 0.318\alpha_{\rm S}\big), \tag{2.25}$$

$$A_{\rm FB}^{(1);T} = A_{\rm FB}^{(0)}\left(1 - \left\{\frac{7}{4} - 4\ln\frac{3}{2} + \frac{\pi^2}{6} + \ln^2 2 - \frac{5}{8}\ln 3 + 2\mathrm{Li}_2\left(-\frac{1}{2}\right)\right\}C_{\rm F}\frac{\alpha_{\rm S}}{\pi}\right) \tag{2.26}$$

$$\simeq A_{\rm FB}^{(0)}\left(1 - 0.670C_{\rm F}\frac{\alpha_{\rm S}}{\pi}\right) \simeq A_{\rm FB}^{(0)}\left(1 - 0.285\alpha_{\rm S}\right). \tag{2.27}$$

The result in eq. (2.25) is well known [3]. The analytical result in eq. (2.26) agrees with the numerical calculation performed in refs. [5, 6]. The difference between the two definitions is only about 0.4% for $\alpha_{\rm S} \sim 0.12$.

We remind the reader that the NLO QCD correction to the symmetric cross section $\sigma_{\rm S}$ in the massless limit is equal to the correction to the $\mathrm{e^+e^-}$ total cross section, namely

$$\sigma_{\rm S} = \sigma_{\rm S}^{(0)}\left(1 + \frac{3}{4}C_{\rm F}\frac{\alpha_{\rm S}}{\pi} + \mathcal{O}(\alpha_{\rm S}^2)\right). \tag{2.28}$$

[4]Note that the relation (2.23) is explicitly violated for massive quarks.

Thus, eqs. (2.25) and (2.26) imply the following results for the antisymmetric cross sections

$$\sigma_{\rm A}^{b} = \sigma_{\rm A}^{(0)} \left(1 + \mathcal{O}(\alpha_{\rm S}^2)\right), \tag{2.29}$$

$$\sigma_{\rm A}^{T} = \sigma_{\rm A}^{(0)} \left(1 - \left\{1 - 4\ln\frac{3}{2} + \frac{\pi^2}{6} + \ln^2 2 - \frac{5}{8}\ln 3 + 2{\rm Li}_2\left(-\frac{1}{2}\right)\right\} C_{\rm F}\frac{\alpha_{\rm S}}{\pi} + \mathcal{O}(\alpha_{\rm S}^2)\right) \tag{2.30}$$

$$\simeq \sigma_{\rm A}^{(0)} \left(1 + 0.034\alpha_{\rm S} + \mathcal{O}(\alpha_{\rm S}^2)\right). \tag{2.31}$$

The vanishing of the $\mathcal{O}(\alpha_{\rm S})$-correction to the antisymmetric cross section $\sigma_{\rm A}^{b}$ with respect to the b-quark axis in the massless case was first noticed in ref. [3].

Unlike at LO, the corrections to $A_{\rm FB}^{(1)}$ due to the finite mass of the b quark are of $\mathcal{O}(m_b/Q)$. The mass corrections have been computed in analytic form for the b-quark direction [4] and numerically for the thrust direction [5].

3. Contributions at next-to-next-to-leading order

At next-to-next-to-leading order (NNLO) we have to consider the diagrams of figures 1–5. The single diagram drawn in figure 1(b) stands for all the one-loop diagrams with one virtual gluon. Analogously, the diagram in figure 3 stands for all the tree-level diagrams contributing to the $b\bar{b}gg$ final state, and so forth.

We separate the contributions to the cross sections into three classes: flavour non-singlet (NS), flavour singlet (S), and interference (or triangle) (Tr). We thus

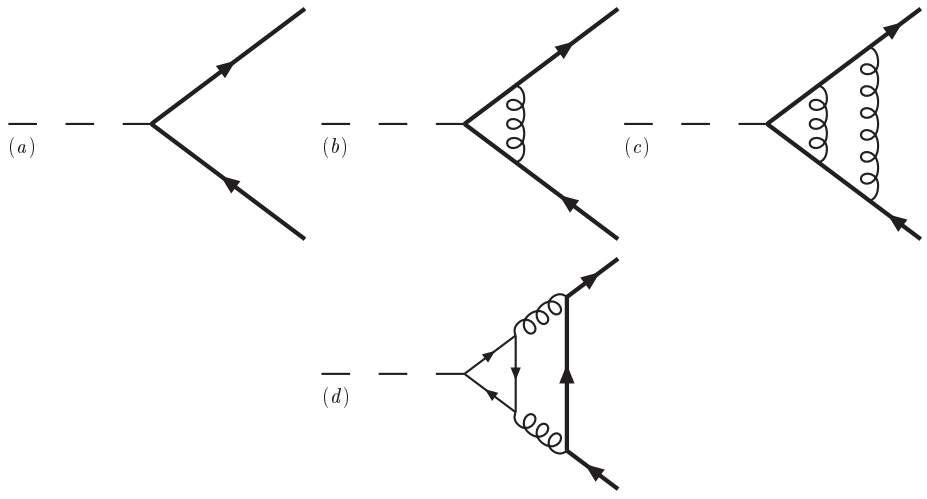

Figure 1: Some of the diagrams contributing to the $b\bar{b}$ final state up to $\mathcal{O}(\alpha_{\rm S}^2)$. The dashed line represents either the axial or vector current, the thick line the b and the thin line another quark q, which must be summed over flavours, including the b- and t-quark contributions.

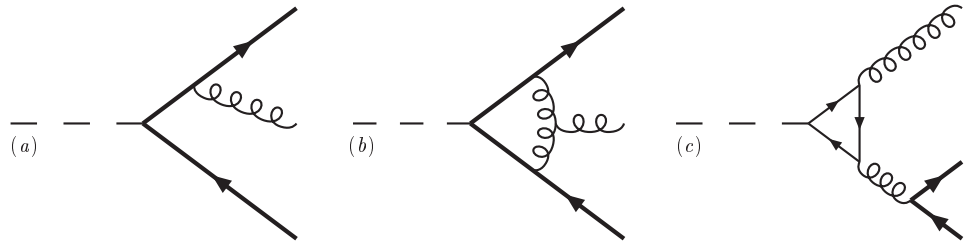

Figure 2: Some of the diagrams contributing to the $b\bar{b}g$ final state up to $\mathcal{O}(\alpha_S^2)$. The dashed line represents either the axial or vector current, the thick line the b and the thin line another quark q, which must be summed over flavours, including the b- and t-quark contributions.

write the cross sections as

$$\sigma_S = \sigma_{S,NS} + \sigma^{(2)}_{S,S} + \sigma^{(2)}_{S,Tr} + \mathcal{O}\left(\alpha_S^3\right), \tag{3.1}$$

$$\sigma_A = \sigma_{A,NS} + \sigma^{(2)}_{A,Tr} + \mathcal{O}\left(\alpha_S^3\right). \tag{3.2}$$

In this notation, up to $\mathcal{O}(\alpha_S)$ there are only non-singlet contributions. Thus, $\sigma^{(2)}_{S,S}$, $\sigma^{(2)}_{S,Tr}$ and $\sigma^{(2)}_{A,Tr}$ are proportional to α_S^2. Note also that there are no singlet contributions to the antisymmetric cross section σ_A.

The forward-backward asymmetry is decomposed in a similar way. Expanding the ratio σ_A/σ_S up to $\mathcal{O}(\alpha_S^2)$, we write

$$A^{(2)}_{FB} = A^{(2)}_{FB,NS} + \frac{\sigma^{(0)}_A}{\sigma^{(0)}_S}\left(\frac{\sigma^{(2)}_{A,Tr}}{\sigma^{(0)}_A} - \frac{\sigma^{(2)}_{S,Tr}}{\sigma^{(0)}_S} - \frac{\sigma^{(2)}_{S,S}}{\sigma^{(0)}_S}\right), \tag{3.3}$$

where $A^{(2)}_{FB,NS}$ denotes the non-singlet component:

$$A^{(2)}_{FB,NS} = \frac{\sigma_{A,NS}}{\sigma_{S,NS}}. \tag{3.4}$$

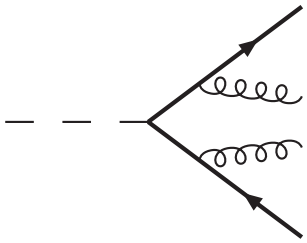

Figure 3: One of the diagrams contributing to the $b\bar{b}gg$ final state at $\mathcal{O}(\alpha_S^2)$. The dashed line represents either the axial or vector current.

We now discuss our treatment of each contribution in turn. The classification of the four-b contribution of figure 5 also warrants additional discussion.

3.1 Triangle contributions

In this class we group all the cross section contributions consisting of two quark triangles, one attached to each current. These correspond to the interference between the diagrams in figures $1(d)$ and $1(a)$, between those in figures $2(c)$ and $2(a)$, and between those in figures $4(b)$ and $4(a)$. They give non-universal (i.e., non-factorizable) corrections to both the symmetric and antisymmetric cross sections. They are calculated in ref. [7] for the b-quark axis definition and found to be very small. To our

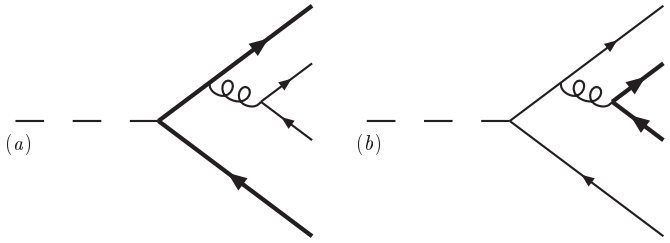

Figure 4: Some of the diagrams contributing to the $b\bar{b}q\bar{q}$ final state at $\mathcal{O}(\alpha_{\rm S}^2)$. The dashed line represents either the axial or vector current, the thick line the b and the thin line some other quark flavour q, with $q \neq b$.

knowledge their contribution to the thrust axis definition has never been calculated, but we expect it to be similarly small. We therefore neglect it, i.e., $\sigma^{(2)}_{{\rm S},Tr}$ and $\sigma^{(2)}_{{\rm A},Tr}$ in eq. (3.3), from our calculation.[5]

3.2 Singlet contributions

In this class we group the square of the diagrams of figure $4(b)$, where the final-state b quark is not coupled to the current. In these contributions the b and $\bar{b}$ are produced in a definite state of charge conjugation, $C = +1$. They therefore cannot contribute to the antisymmetric cross section, $\sigma_{\rm A}$. Their contribution to the symmetric cross section, $\sigma_{\rm S}$, is logarithmically enhanced in the small-mass limit and proportional to $\alpha_{\rm S}^2 \ln^3 Q^2/m_b^2$. An approximate expression for it, denoted by $F^{\rm Branco}$, was used in ref. [7]. It is calculated exactly to $\mathcal{O}(\alpha_{\rm S}^2)$ in refs. [10, 11], and the leading and next-to-leading logarithms are summed to all orders in $\alpha_{\rm S}$ in ref. [11].

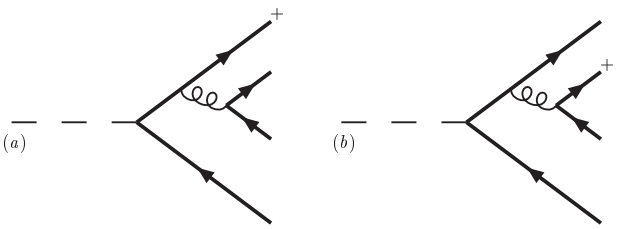

Figure 5: One of the diagrams contributing to the $b\bar{b}b\bar{b}$ final state at $\mathcal{O}(\alpha_{\rm S}^2)$. The dashed line represents either the axial or vector current. The cross indicates which of the two b quarks is triggered on: both contributions must be summed.

Note that the singlet contributions to $\sigma_{\rm S}$ include an additional term coming from the $b\bar{b}b\bar{b}$ final state. As discussed in section 3.3, this term is very similar to that described above. It was missing in the expression denoted by $F^{\rm Branco}$ in ref. [7].

In some sense the singlet component is a 'background' to the forward-backward asymmetry measurement and, in fact, in the experimental analyses (see, e.g., ref. [12]) it is statistically subtracted using Monte Carlo event generators. We therefore neglect it, i.e., $\sigma^{(2)}_{{\rm S},S}$ in eq. (3.3), from our calculation.

[5] We remind the reader that the triangle contributions to both $\sigma_{\rm S}$ and $\sigma_{\rm A}$ are finite in the massless limit $m_b \to 0$, provided that the sums over quark flavour q in the diagrams of figures $1(d)$ and $2(c)$ run over complete SU(2) doublets.

3.3 Four-b contributions

The classification of the four-b diagrams of figure 5 deserves special mention. Let us first point out a basic fact. The four-b diagrams of figure 5 contribute to both the b-quark cross sections $\sigma_{\rm S}$ and $\sigma_{\rm A}$ and the e^+e^- total cross section. However, they appear with different multiplicity factors in the two cases. In the case of the e^+e^- total cross section the multiplicity factor is simply equal to unity. In the contribution to the *inclusive* b-quark cross sections $\sigma_{\rm S}$ and $\sigma_{\rm A}$, these diagrams count twice since there are two b quarks in the final state. This observation is relevant in the discussion that follows and, in particular, it is important in understanding the results for the non-singlet component of the symmetric cross section $\sigma_{\rm S}$ discussed in section 3.4.

After summing and squaring the diagrams in figure 5, we obtain two types of contribution: (i) those that are identical to the contributions of figure 4 but with the other quark q replaced by an untriggered-on b quark, and (ii) those that are genuine interference terms arising from the fact that the two antiquarks are indistinguishable, called the E-term in ref. [13]. The squared diagrams of type (i) are treated as those of figure 4, that is, we lump them together with the corresponding terms from figure 4 in the singlet ($\sigma^{(2)}_{{\rm S},S}$ in eq. (3.1), non-singlet ($\sigma_{{\rm S},NS}$ and $\sigma_{{\rm A},NS}$ in eqs. (3.1) and (3.2) or triangle ($\sigma^{(2)}_{{\rm S},Tr}$ and $\sigma^{(2)}_{{\rm A},Tr}$ in eqs. (3.1) and (3.2) contributions. The squared diagrams of type (ii), which give a universal (i.e., factorizable) correction to both the antisymmetric and symmetric cross sections, can be considered part of the non-singlet contributions.

It is not entirely clear how four-quark final states are actually treated in the different experimental analyses, i.e., the extent to which they are genuinely measuring the inclusive cross sections. Often some vague statement like "a four-b final state is more likely to be tagged than a two-b one, but less than twice as likely" is made. To know what to calculate one must understand the corrections that are applied for this difference in tagging efficiency, which are not usually explicitly stated in the papers. In the absence of a unique experimental procedure and of a definitive statement from the experiments on what they are measuring, we make this ambiguity explicit by multiplying the E-term by an arbitrary weight factor W_E.[6] An inclusive definition would correspond to $W_E = 2$ (each b quark contributing once), while an exclusive definition (the cross section for events containing at least one b quark) would correspond to $W_E = 1$. Since the forward-backward asymmetry is defined to be the asymmetry of a differential cross section, it is clear that we must use the same cross section definition in the numerator and denominator,

[6]Note that we use the same normalization as in ref. [13] (see also eq. (B.1)) in which the E-term already includes an identical-particle factor of $1/(2!)^2$ because there are two identical quarks and two identical antiquarks in the final state. Thus, when we set $W_E = 2$ we actually include an overall factor of $W_E/(2!)^2 = 1/2!$.

i.e. that W_E must be the same in the symmetric and antisymmetric cross sections.

We return to the rôle of the weight factor W_E after discussing the general form of the non-singlet contributions.

3.4 Non-singlet contributions

Here we consider all the other contributions that have not yet been treated, namely all the diagrams in figure 1 except those in figure 1(d), the diagrams in figures 2(a), 2(b), 3, 4(a) and 5(a), as well as the E-term defined above. All these terms are included in the non-singlet components $\sigma_{\mathrm{S},NS}$ and $\sigma_{\mathrm{A},NS}$ of eqs. (3.1) and (3.2). Actually, introducing the weight factor W_E for the E-term, we can define the following symmetric and antisymmetric cross sections

$$\sigma_{\mathrm{S},NS}(W_E) = \sigma_{\mathrm{S},NS}(W_E = 0) + W_E \sigma_S^{(0)} \int E_{\mathrm{S}} \,, \tag{3.5}$$

$$\sigma_{\mathrm{A},NS}(W_E) = \sigma_{\mathrm{A},NS}(W_E = 0) + W_E \sigma_{\mathrm{A}}^{(0)} \int E_{\mathrm{A}} \,, \tag{3.6}$$

where $\int E_{\mathrm{S}}$ and $\int E_{\mathrm{A}}$ denote the integral of the symmetric and antisymmetric E-term, respectively. We recall that the 'truly' inclusive cross sections in eq. (2.4) correspond to the definition with $W_E = 2$, i.e., $\sigma_{\mathrm{S},NS} = \sigma_{\mathrm{S},NS}(W_E = 2)$ and $\sigma_{\mathrm{A},NS} = \sigma_{\mathrm{A},NS}(W_E = 2)$.

The $\mathcal{O}(\alpha_{\mathrm{S}}^2)$-calculation of the cross sections in eqs. (3.5), (3.6) and of the corresponding forward-backward asymmetry in the case of a finite b-quark mass is extremely complicated, and we are not able to perform it. It is thus convenient to separate the calculation into a piece that is finite in the massless limit and a simpler piece that is not. Then, the (although, cumbersome) finite piece can be more easily computed in the massless approximation, while the simpler non-finite piece can be computed in the massive theory.

It is possible to show (appendix A) that the inclusive definition, with $W_E = 2$, results in an antisymmetric cross section σ_{A} (or, analogously, $\sigma_{\mathrm{A},NS}$) that is finite in the massless limit, at least at $\mathcal{O}(\alpha_{\mathrm{S}}^2)$. However, in the same limit, the inclusive symmetric cross section is divergent at $\mathcal{O}(\alpha_{\mathrm{S}}^2)$, even if we only consider its non-singlet component. The corrections to (the non-singlet component of) the forward-backward asymmetry itself must therefore also be divergent in the massless limit.

This final statement remains true for *any* value of $W_E > 0$. For example, with $W_E = 1$, the non-singlet part of the symmetric cross section is finite (see eq. (3.10)), but the antisymmetric cross section contains logarithmically-enhanced terms.

The divergences in the non-singlet components correspond to logarithmically-enhanced terms $\alpha_{\mathrm{S}}^2 \ln Q^2/m_b^2$ coming from the E-term in the triple-collinear limit, i.e., when three fermions of the four-quark final state become simultaneously parallel (appendix B). The integral of the symmetric E-term is calculated for finite values of

the quark mass in appendix B. Neglecting corrections of $\mathcal{O}(m_b/Q)$, the final result is

$$\int E_{\rm S} = C_{\rm F}\left(C_{\rm F} - \frac{C_{\rm A}}{2}\right)\left(\frac{\alpha_{\rm S}}{2\pi}\right)^2\left[2\left(\frac{13}{4} - \frac{\pi^2}{2} + 2\zeta_3\right)\ln\frac{Q^2}{m_b^2} - 8.1790 \pm 0.0013\right]. \tag{3.7}$$

As expected from the singular behaviour in the triple-collinear limit, the analytic coefficient in front of $\ln Q^2/m_b^2$ is proportional to the integral of the non-singlet Altarelli-Parisi probability $P_{q\bar{q}}^{NS}(z,\alpha_{\rm S})$ (see, for instance, the first paper in ref. [14]):

$$\int_0^1 dz P_{q\bar{q}}^{NS}(z,\alpha_{\rm S}) = \left(\frac{\alpha_{\rm S}}{2\pi}\right)^2 C_{\rm F}\left(C_{\rm F} - \frac{1}{2}C_{\rm A}\right)\left(\frac{13}{4} - \frac{\pi^2}{2} + 2\zeta_3\right), \tag{3.8}$$

$$\simeq \left(\frac{\alpha_{\rm S}}{2\pi}\right)^2 C_{\rm F}\left(C_{\rm F} - \frac{1}{2}C_{\rm A}\right)0.7193\,. \tag{3.9}$$

The constant term in the square bracket on the right-hand side of eq. (3.7) is the result of our numerical calculation.

Having pointed out that the symmetric E-term is divergent in the massless limit, it is very simple to show how the divergence appears in the inclusive symmetric cross section. According to the definition of the non-singlet component of σ_S, the virtual diagrams that contribute to $\sigma_{{\rm S},NS}$ are exactly those that contribute to the $\mathrm{e^+e^-}$ total cross section. As for the real diagrams, they only differ by the contributions coming from the E-term. In the total cross section, the E-term enters with a multiplicity factor $W_E = 1$, and its divergence is cancelled by that of the virtual diagrams. In the inclusive b-quark cross section, the multiplicity factor of the E-term is $W_E = 2$ and, thus, the cancellation of the divergence with the virtual terms is spoiled.

This argument also allows us to directly compute the $\mathcal{O}(\alpha_{\rm S}^2)$-correction to eq. (3.5). Exploiting the fact that the massless QCD correction to $\sigma_{{\rm S},NS}(W_E = 1)$ is equal to the correction $R_{\mathrm{e^+e^-}}$ to the total cross section, we write

$$\sigma_{{\rm S},NS}(W_E = 1) = \sigma_S^{(0)}\Big[R_{\mathrm{e^+e^-}} + \mathcal{O}\big(\alpha_{\rm S}^3\big)\Big], \tag{3.10}$$

and, more generally,

$$\sigma_{{\rm S},NS}(W_E) = \sigma_{\rm S}^{(0)}\left[R_{\mathrm{e^+e^-}} + (W_E - 1)\int E_{\rm S} + \mathcal{O}\big(\alpha_{\rm S}^3\big)\right]. \tag{3.11}$$

Then, we obtain an explicit expression for $\sigma_{{\rm S},NS}(W_E)$ by simply introducing in eq. (3.11) our result in eq. (3.7) for $\int E_{\rm S}$ and the well-known result [15] for $R_{\mathrm{e^+e^-}}$:

$$R_{\mathrm{e^+e^-}} = 1 + \frac{3}{4}C_{\rm F}\frac{\alpha_{\rm S}(Q^2)}{\pi} + \left(\frac{\alpha_{\rm S}(Q^2)}{2\pi}\right)^2 \times \tag{3.12}$$

$$\times\, C_{\rm F}\left\{-\frac{3}{8}C_{\rm F} + C_{\rm A}\left(\frac{123}{8} - 11\zeta_3\right) + T_{\rm R}N_f\left(4\zeta_3 - \frac{11}{2}\right)\right\} + \mathcal{O}\big(\alpha_{\rm S}^3\big)\,, \tag{3.13}$$

where $T_{\rm R} = 1/2$ and N_f is the number of light flavours (e.g., $N_f = 5$ at LEP).

In particular, for the inclusive symmetric cross section we obtain

$$\sigma_{\mathrm{S},NS} = \sigma_{\mathrm{S},NS}(W_E = 2) = \sigma_S^{(0)} \left[R_{\mathrm{e^+e^-}} + \int E_{\mathrm{S}} + \mathcal{O}\big(\alpha_{\mathrm{S}}^3\big) \right] . \tag{3.14}$$

The explicit $\mathcal{O}(\alpha_{\mathrm{S}}^2)$-calculation of the antisymmetric cross section $\sigma_{\mathrm{A},NS}$ and of the forward-backward asymmetry is described in the next section.

Note that our result in eq. (3.14) for the inclusive symmetric cross section disagrees with the corresponding result of Ravindran and van Neerven [8]. Their expression for the correction to the symmetric cross section ($f_{\mathrm{T}} + f_{\mathrm{L}}$ in their eqs. (31) and (32)) is equal to the result in eq. (3.13) for the $\mathcal{O}(\alpha_{\mathrm{S}}^2)$-correction to $R_{\mathrm{e^+e^-}}$. The disagreement thus regards the additional logarithmically-enhanced term $\int E_{\mathrm{S}}$ included in our expression. The multiplicity of b-quarks is not required to be finite in massless QCD (even in the non-singlet sector), and thus we cannot find any reason why this logarithmically-enhanced term can disappear from the inclusive symmetric cross section.

The results of ref. [8] for $\sigma_{\mathrm{S},NS} = \sigma_{\mathrm{S},NS}(W_E = 2)$ are based on the calculation of the single-particle inclusive distribution performed in refs. [16]. Our result is consistent with those in refs. [16]. In fact, we have evaluated the integral over the longitudinal-momentum fraction z of the non-singlet coefficient function $C_{\mathrm{S},q}^{NS}(z, \alpha_{\mathrm{S}}(Q^2), Q^2/\mu_{\mathrm{F}}^2) = C_{\mathrm{T},q}^{NS} + C_{L,q}^{NS}$, computed there. This integral is proportional to $\sigma_{\mathrm{S},NS} = \sigma_{S,NS}(W_E = 2)$ in massless QCD after factorization of collinearly-divergent contributions at the factorization scale μ_{F}. We find that the integral explicitly depends on $\ln Q^2/\mu_{\mathrm{F}}^2$, thus proving that $\sigma_{S,NS}$ is not finite in massless QCD. The coefficient of $\ln Q^2/\mu_{\mathrm{F}}^2$ exactly agrees with the coefficient of $\ln Q^2/m_b^2$ in our eqs. (3.7) and (3.14).

4. Calculation of the non-singlet contribution at $\mathcal{O}(\alpha_{\mathrm{S}}^2)$

As discussed in section 3.4, the NNLO corrections to the non-singlet component of the forward-backward asymmetry, $A_{\mathrm{FB},NS}$, are divergent in the massless limit. The divergent behaviour remains true also if we abandon the fully inclusive definition by introducing the arbitrary weight W_E for the E-term. Thus, $A_{\mathrm{FB},NS}$ cannot be computed at $\mathcal{O}(\alpha_{\mathrm{S}}^2)$ by using the massless approximation.

Nonetheless, since both $\sigma_{\mathrm{A},NS}(W_E = 2)$ and $\sigma_{\mathrm{S},NS}(W_E = 1)$ are finite when $m_b \to 0$, we can use the dependence on W_E to construct an unphysical observable that is finite in the massless limit:

$$A_{\mathrm{FB}}^{(2);\mathrm{finite}} \equiv \frac{\sigma_{\mathrm{A},NS}(W_E = 2)}{\sigma_{\mathrm{S},NS}(W_E = 1)} . \tag{4.1}$$

The physical result for $W_E = 2$ is then given by

$$A_{\mathrm{FB},NS}^{(2)} = A_{\mathrm{FB}}^{(2);\mathrm{finite}} - \frac{\sigma_{\mathrm{A}}^{(0)}}{\sigma_{\mathrm{S}}^{(0)}} \int E_{\mathrm{S}} = A_{\mathrm{FB}}^{(2);\mathrm{finite}} - A_{\mathrm{FB}}^{(0)} \int E_{\mathrm{S}} \, , \tag{4.2}$$

where $\int E_{\rm S}$ is the integral of the symmetric E-term, given in eq. (3.7).

The massless calculation of $A_{\rm FB}^{(2);\rm finite}$ can be performed in a similar way to the NLO calculation of section 2.2. The total contribution can be written as

$$A_{\rm FB}^{(2);\rm finite} = \frac{\sigma_{\rm A}^{(0)} + \sigma_{\rm A}^{(1)} + \sigma_{\rm A}^{(2);\text{two-loop}} + \sigma_{\rm A}^{(2);\text{one-loop}} + \sigma_{\rm A}^{(2);\rm tree}(W_E = 2)}{\sigma_{\rm S}^{(0)} + \sigma_{\rm S}^{(1)} + \sigma_{\rm S}^{(2);\text{two-loop}} + \sigma_{\rm S}^{(2);\text{one-loop}} + \sigma_{\rm S}^{(2);\rm tree}(W_E = 1)}\,, \tag{4.3}$$

where $\sigma_{\rm A}^{(1)}$ and $\sigma_{\rm S}^{(1)}$ are the complete contributions to the antisymmetric and symmetric cross sections at $\mathcal{O}(\alpha_{\rm S})$. The non-singlet $\mathcal{O}(\alpha_{\rm S}^2)$-contributions from the two-parton, three-parton and four-parton final states are denoted by $\sigma^{(2);\text{two-loop}}$, $\sigma^{(2);\text{one-loop}}$ and $\sigma^{(2);\rm tree}$ respectively. Of course, the dependence on W_E enters only through the four-parton terms $\sigma_{\rm A}^{(2);\rm tree}(W_E = 2)$ and $\sigma_{\rm S}^{(2);\rm tree}(W_E = 1)$.

If we continue to use a regularization scheme that preserves the helicity conservation of massless QCD, like dimensional regularization, the two-loop corrections are again proportional to the tree-level results

$$\frac{\sigma_{\rm A}^{(2);\text{two-loop}}}{\sigma_{\rm A}^{(0)}} = \frac{\sigma_{\rm S}^{(2);\text{two-loop}}}{\sigma_{\rm S}^{(0)}}\,, \tag{4.4}$$

so that if we expand the ratio in eq. (4.3) up to $\mathcal{O}(\alpha_{\rm S}^2)$, the two-loop corrections cancel, and we obtain

$$\begin{aligned} A_{\rm FB}^{(2);\rm finite} = \frac{\sigma_{\rm A}^{(0)}}{\sigma_{\rm S}^{(0)}}\Bigg[1 + \left(1 - \frac{\sigma_{\rm S}^{(1)}}{\sigma_{\rm S}^{(0)}}\right)\left(\frac{\sigma_{\rm A}^{(1)}}{\sigma_{\rm A}^{(0)}} - \frac{\sigma_{\rm S}^{(1)}}{\sigma_{\rm S}^{(0)}}\right) + \frac{\sigma_{\rm A}^{(2);\text{one-loop}}}{\sigma_{\rm A}^{(0)}} - \\ - \frac{\sigma_{\rm S}^{(2);\text{one-loop}}}{\sigma_{\rm S}^{(0)}} + \frac{\sigma_{\rm A}^{(2);\rm tree}(W_E = 2)}{\sigma_{\rm A}^{(0)}} - \frac{\sigma_{\rm S}^{(2);\rm tree}(W_E = 1)}{\sigma_{\rm S}^{(0)}}\Bigg]\,. \end{aligned} \tag{4.5}$$

The first line can be calculated analytically (see section 2.2), but the second line is too complicated to be able to, so must be done numerically. Since the two-loop terms have cancelled, this has the structure of a NLO three-jet calculation, as first noticed by Altarelli and Lampe [7]. Thus the calculation can be performed using known techniques (we use the dipole-formalism version of the subtraction method [17]). One simply has to replace the full matrix element squared by the appropriate contractions of the hadronic tensor, as in eqs. (2.6) and (2.7). We have obtained simplified analytical expressions for these contractions by using the matrix elements originally computed by the Leiden group [18]. We have also checked that these expressions numerically agree with the code of ref. [19].

4.1 Numerical results

We are finally ready to present our numerical results. We start with the unphysical, but finite, quantity defined in eq. (4.1), and separate out the different colour factors,

b-quark axis	C	N	T
AL [7]	4.4 ± 0.5	-10.3 ± 0.3	5.68 ± 0.04
RvN [8]	$\frac{3}{8} = 0.375$	$-\frac{123}{8} = -15.375$	$\frac{11}{2} = 5.5$
Our Calculation	0.3765 ± 0.0038	-15.3769 ± 0.0034	5.5002 ± 0.0008

Table 1: Results for the coefficients of the $\mathcal{O}(\alpha_S^2)$ correction to the finite part of the forward-backward asymmetry with the b-quark axis definition, eqs. (4.2) and (4.6).

as in refs. [7, 8]:

$$A_{\rm FB}^{(2);{\rm finite};b} = A_{\rm FB}^{(0)}\Bigg[1 - \frac{\alpha_S}{2\pi}\left(1 - \frac{\alpha_S}{2\pi}\frac{3}{2}C_F\right)\left(\frac{3}{2}C_F\right) + \\ + \left(\frac{\alpha_S}{2\pi}\right)^2 C_F\left(CC_F + NN_C + TT_R N_f\right)\Bigg], \tag{4.6}$$

with $\alpha_S \equiv \alpha_S(Q^2)$. Our numerical results are shown in table 1, in comparison with the previous calculations. It is clear that we disagree badly with the results of Altarelli and Lampe [7], but are in excellent agreement with Ravindran and van Neerven [8], who give the coefficients analytically. However, we should recall that this must have subtracted from it the logarithmically-enhanced term of eqs. (4.2) and (3.7), which is not present in the result of ref. [8]. In fact, in section 3.4 we have already pointed out that their expression for the correction to the symmetric cross section does not agree with ours, but, rather, it is actually equal to our $\sigma_{S,NS}^{(2)}(W_E = 1)$. So, the fact that their result for the complete $A_{\rm FB}^{(2)}$ agrees with our $A_{\rm FB}^{(2);{\rm finite}}$ means that we confirm their result [20, 8] for the inclusive antisymmetric cross section $\sigma_A^{(2)} = \sigma_A^{(2)}(W_E = 2)$ (f_A in equation (33) of ref. [8]).

The disagreement with the result of ref. [7] may be related to the poor numerical convergence of their calculational method (i.e., the effect of large numerical cancellations).

Using our numerical program it is straightforward to calculate the forward-backward asymmetry with any other axis definition (or cuts, for example on the value of the thrust). With the thrust axis definition, we obtain

$$A_{\rm FB}^{(2);{\rm finite};T} = A_{\rm FB}^{(0)}\Bigg[1 - \frac{\alpha_S}{2\pi}\big(1 - \frac{\alpha_S}{2\pi}\frac{3}{2}C_F\big)\left(1.34C_F\right) + \\ + \left(\frac{\alpha_S}{2\pi}\right)^2 C_F\left(CC_F + NN_C + TT_R N_f\right)\Bigg], \tag{4.7}$$

with $\alpha_S \equiv \alpha_S(Q^2)$ and the coefficients given in table 2. The logarithmically-enhanced piece that has to be added to this is identical to that in the b-quark axis definition, namely eqs. (4.2), (3.7). It is worth noting that the difference between the two definitions is the same size and in the same direction as at $\mathcal{O}(\alpha_S)$, leading to an overall difference of 0.8% for $\alpha_S \sim 0.12$.

thrust axis	C	N	T
Our Calculation	-3.7212 ± 0.0065	-9.6011 ± 0.0049	4.4144 ± 0.0006

Table 2: Results for the coefficients of the $\mathcal{O}(\alpha_S^2)$ correction to the finite part of the forward-backward asymmetry with the thrust axis definition, eqs. (4.2) and (4.7).

Since $A_{FB}^{(2);\text{finite};T}$ is defined by the ratio in eq. (4.1), using the expression in eq. (3.10) for $\sigma_{S,NS}(W_E = 1)$, we can translate our result in eq. (4.7) into an equivalent result for the antisymmetric cross section defined with respect to the thrust axis. We have:

$$\sigma_{A,NS}^T = \sigma_A^{(0)} \Bigg\{ 1 + 0.034\alpha_S(Q^2) + \left(\frac{\alpha_S(Q^2)}{2\pi}\right)^2 C_F \left[\left(-\frac{3}{8} + C\right) C_F + \right.$$
$$\left. + \left(\frac{123}{8} - 11\zeta_3 + N\right) C_A + \left(4\zeta_3 - \frac{11}{2} + T\right) T_R N_f \right] + \mathcal{O}\left(\alpha_S^3\right) \Bigg\}. \tag{4.8}$$

with the coefficients C, N and T given in table 2.[7]

We finally recall that we include an arbitrary factor W_E in front of the four-b contribution to account for the way in which it is treated in the experimental analyses. For a fully inclusive definition, in which each b quark contributes once, W_E should be set equal to 2, while for an exclusive definition, W_E should be set equal to 1. Our final result for the non-singlet component of the forward-backward asymmetry, is then:

$$A_{FB,NS}^{(2)}(W_E) \equiv \frac{\sigma_{A,NS}(W_E)}{\sigma_{S,NS}(W_E)} =$$
$$= A_{FB}^{(2);\text{finite}} - A_{FB}^{(0)} \left[\left(1 - \frac{1}{2}W_E\right) \left(2\int E_A - \int E_S\right) + \frac{1}{2}W_E \int E_S \right], \tag{4.9}$$

where $A_{FB}^{(2);\text{finite}}$ is given in eqs. (4.6), (4.7) and tables 1 and 2, $\int E_S$ is given in eq. (3.7) and (see appendix B)

$$2\int E_A - \int E_S = \left(\frac{\alpha_S}{2\pi}\right)^2 C_F \left(C_F - \frac{1}{2}C_A\right)\left(0.3620 \pm 0.0007\right), \quad \text{quark axis}, \tag{4.10}$$
$$2\int E_A - \int E_S = \left(\frac{\alpha_S}{2\pi}\right)^2 C_F \left(C_F - \frac{1}{2}C_A\right)\left(0.1144 \pm 0.0009\right), \quad \text{thrust axis}. \tag{4.11}$$

Note that the combinations of E-term contributions in eqs. (4.10) and 4.11 are finite in the massless limit (see the discussion in appendix B).

[7] In the analogous expression for $\sigma_{A,NS}^b$, the coefficient of $\alpha_S(Q^2)$ vanishes and C, N and T are those given in table 1, which exactly cancel the rational numbers in eq. (4.8), leaving only $3\beta_0\zeta_3$, with $\beta_0 = \frac{11}{3}C_A - \frac{4}{3}T_R N_f$, as pointed out in ref. [20].

	AL [7] quark axis	RvN [8] quark axis	Our calculation quark axis	Our calculation thrust axis
Correction, $A_{\rm FB}^{(2)}/A_{\rm FB}^{(0)}$	0.962	0.952	0.952	0.956

Table 3: Total QCD correction to the forward-backward asymmetry in the small-mass limit, with $\alpha_{\rm S} = 0.12$. In each case, the thrust axis definition is used for the $\mathcal{O}(\alpha_{\rm S})$ correction and the definition shown is used for the $\mathcal{O}(\alpha_{\rm S}^2)$ correction, as discussed in the text.

Putting all these numbers together, and setting $N_f = 5$, we write the forward-backward asymmetry according to the two definitions as:

$$A_{{\rm FB},NS}^{(2);b}(W_E) = A_{\rm FB}^{(0)}\left[1 - 0.318\alpha_{\rm S} - 0.973\alpha_{\rm S}^2 + W_E\alpha_{\rm S}^2\left(0.00405\ln\frac{Q^2}{m_b^2} - 0.0240\right)\right], \tag{4.12}$$

$$A_{{\rm FB},NS}^{(2);T}(W_E) = A_{\rm FB}^{(0)}\left[1 - 0.284\alpha_{\rm S} - 0.676\alpha_{\rm S}^2 + W_E\alpha_{\rm S}^2\left(0.00405\ln\frac{Q^2}{m_b^2} - 0.0233\right)\right]. \tag{4.13}$$

5. Conclusion

We have calculated the second-order corrections to the non-singlet component of the forward-backward asymmetry in e^+e^- annihilation. We have retained all terms that do not vanish in the small-mass limit (constants and logarithmically-enhanced terms). Our result is also valid for the left-right forward-backward asymmetry.

Using the quark axis definition we do not agree with any existing calculation. Separating the asymmetry into its symmetric and antisymmetric parts, we find that we agree with Ravindran and van Neerven [8] for the antisymmetric part, which is finite in massless QCD. For the symmetric part we disagree by a term that is divergent in massless QCD, so is logarithmically-enhanced in the full theory.

We have obtained results for the first time with the thrust axis definition, which is actually what is used in the experimental measurements. After including the second-order contributions, the difference between the two axis definitions is twice as large as at first order, amounting to 0.8%.

We summarize the total QCD correction according to the various available calculations in table 3. We continue to neglect all terms that vanish in the massless limit, and discuss the effect of mass corrections below. Since in the existing experimental analyses (see for example ref. [12]), the known $\mathcal{O}(\alpha_{\rm S})$ correction for the thrust axis definition was included, together with the Altarelli and Lampe quark axis value for the $\mathcal{O}(\alpha_{\rm S}^2)$ corrections, we do the same in table 3.

We find that the difference between the Ravindran and van Neerven calculation and ours is numerically irrelevant, being smaller than 10^{-4} for b quarks and $\sim 2.5 \times 10^{-4}$ for c quarks. Therefore at the numerical precision required by current

or any foreseen experiments, we agree with their result—the difference is only one of principle. The difference between the Altarelli and Lampe calculation and ours for the quark axis definition is more significant though, at around 1%. However, the error in their calculation and the effect of using the thrust axis definition partially cancel, and the total difference is around 0.6%.

Before quantifying the impact of these differences, we mention the important fact, discussed in ref. [12], that the experimental procedures introduce a bias towards more two-jet-like events. This actually decreases the size of the QCD corrections considerably, so our numbers should be considered as upper bounds. In fact at present the effect of this bias is typically taken into account using Monte Carlo event generators. Using our numerical calculation, it is straightforward to apply any infrared-safe cuts, for example on the thrust of the event (this effect was first considered at $\mathcal{O}(\alpha_S)$ in ref. [5]). This could be used to reduce the reliance on the generators, or at the least to calibrate their reliability.

To quantify the impact of the differences shown in table 3, we recall a few figures from the latest global electroweak fit [1]. The total error on the LEP average forward-backward asymmetry of b-quarks A_{FB} is 2.1%. The second-order QCD corrections are used to convert the measured value into a measurement of the tree-level asymmetry, $A_{FB}^{(0)}$, at present using the Altarelli and Lampe result. This is then used as input into the fit for the effective weak mixing angle, $\sin^2\theta_{\text{eff}}$, and eventually into the global fit to all electroweak data. Following through this process, our smaller value of the correction in table 3 results in a larger value of $A_{FB}^{(0)}$ and hence a smaller value of $\sin^2\theta_{\text{eff}}$, by about a third of its experimental error.

This has a direct bearing on the fitted value of the Higgs mass, (see figure 9 of ref. [1]). To find the effect of using our corrections would require a complete refitting of all the electroweak data. However, we can get a rough idea simply by fitting the data in figure 9 of ref. [1] alone. We find a roughly linear relation: for each *per mille* that the corrected value of the quark asymmetries is *increased*, we obtain a *per cent decrease* in the central value of the Higgs mass (and its upper bound). Therefore with our 0.6% difference, we expect a reduction of about 5 GeV in the central value. While this is certainly not statistically significant, given the importance that some people attach to this value, it is not irrelevant either.

In trying to estimate the remaining uncertainties in the forward-backward asymmetry, we recall the ingredients still missing from our analysis. We should bear in mind that while the 2% precision of current experiments is close to their final limit, a future linear collider could be capable of experimental errors on the left-right forward-backward asymmetry of order 0.1% [2].

Within small-mass perturbation theory, the first terms that we neglect are $\mathcal{O}(\alpha_S^3)$. To estimate their size, we assume that the coefficient grows as much in going from $\mathcal{O}(\alpha_S^2)$ to $\mathcal{O}(\alpha_S^3)$ as it did from $\mathcal{O}(\alpha_S)$ to $\mathcal{O}(\alpha_S^2)$, and get 0.3%. The more conven-

tional method, varying the renormalization scale from $Q/2$ to $2Q$ results in a similar estimate of 0.2%. A variation in the input value of α_S of ± 0.004 gives only 0.1%.

Within the $\mathcal{O}(\alpha_S^2)$ calculation, we neglected the effect of triangle diagrams. For the quark axis definition, these were calculated in ref. [7], and amount to about 0.1%. We have no reason to suppose they would be larger for the thrust axis definition, and in any case it would not be difficult to calculate them.

We have also neglected linear mass corrections of the type m_b/Q, which are absent at tree level, but arise at higher orders. The full mass correction at $\mathcal{O}(\alpha_S)$ is well known, and is reasonably well approximated by its leading term, $4C_F\alpha_S/\pi m_b/Q$. Since we do not have any higher order corrections to this linear mass term, its renormalization group dependence is not under control, so to estimate the effect of higher order corrections, we vary m_b from its running value in the $\overline{\text{MS}}$ scheme (~ 3 GeV) to its pole value (~ 5 GeV), resulting in a 0.4% variation in A_{FB}.

Finally, at higher orders it is quite possible that the leading mass term could become logarithmically enhanced, for instance, as $\sim \alpha_S^2 m_b/Q \ln^n(Q^2/m_b^2)$ at the second order. Terms like this certainly arise with $n = 1$ simply from the renormalization group effects just mentioned, but the question is whether additional terms can arise from other dynamic effects. A possible additional source of single-logarithmic enhancement is collinear emission, as in the case of the E-term contributions discussed earlier. Owing to the inclusiveness of the forward-backward asymmetry with respect to soft emission, we think that higher powers of logs are unlikely to be present in the non-singlet component at $\mathcal{O}(\alpha_S^2)$. Although this point deserves further investigation, assuming $n \leq 1$ we estimate a resulting uncertainty of 0.5%.

We have not made any attempt to estimate the uncertainty due to non-perturbative corrections. In ref. [12], this is done using Monte Carlo event generators. They find a correction of 0.25% and conservatively assign the whole of this as a systematic error.

To summarize, there are several sources of uncertainty that all contribute at the few per mille level. While this is certainly sufficient for the current precision of the data, matching the precision of a future linear collider measurement could be extremely difficult. It is likely that this could only be done by making even more stringent two-jet cuts in order to work in a region in which the corrections and their uncertainties are smaller.

Acknowledgments

We are grateful to Guido Altarelli, Klaus Mönig and especially Willy van Neerven for discussions of the forward-backward asymmetry and comments on the manuscript. MHS gratefully acknowledges the hospitality of the Theoretical Physics Department of Lund University during the completion of this work.

A. The antisymmetric cross section in massless QCD

In this appendix we show that, up to $\mathcal{O}(\alpha_{\rm S}^2)$, the perturbative-QCD corrections to the heavy-quark antisymmetric cross section $\sigma_{\rm A}$ are finite in the limit of vanishing quark masses.

We are interested in the analogue of the cross section in eq. (2.2) for the inclusive process $\mathrm{e}^+\mathrm{e}^- \to a + X$ where $a = q_f, \bar{q}_f, g$ denotes a generic massless QCD parton. We thus define the antisymmetric[8] cross section $d\sigma_{\rm A}^a/dx$ as follows

$$\frac{d\sigma_{\rm A}^a}{dx} = \int_0^1 d\cos\theta \frac{d\sigma(\mathrm{e}^+\mathrm{e}^- \to a + X)}{dx\, d\cos\theta} - \int_{-1}^0 d\cos\theta \frac{d\sigma(\mathrm{e}^+\mathrm{e}^- \to a + X)}{dx\, d\cos\theta}\,. \tag{A.1}$$

It is also convenient to introduce the N-moments $\sigma_{A,N}^a$ defined by

$$\sigma_{A,N}^a = \int_0^1 dx\, x^{N-1} \frac{d\sigma_{\rm A}^a}{dx}\,, \tag{A.2}$$

and likewise for any other function of the energy fraction x. Note that the massless limit of the b-quark antisymmetric cross section in eq. (2.4) coincides with the $N = 1$ moment of $d\sigma_A^{q_f}/dx$, i.e., $\sigma_{\rm A} = \sigma_{A,N=1}^{q_f}$.

Since we are working in massless QCD, the antisymmetric cross section $d\sigma_{\rm A}^a/dx$ is not finite in perturbation theory and, more precisely, it is collinear divergent. Nonetheless, because of the factorization theorem of mass singularities, once the divergences have been regularized (by using, for instance, dimensional regularization) they can be factorized. The N-moments can be written as

$$\sigma_{A,N}^a = \sum_{b=q_f,\bar{q}_f,g} \hat{\sigma}_{A,N}^b \Gamma_{ba,N}\,, \tag{A.3}$$

where $\hat{\sigma}_{A,N}^b$ is a finite contribution to the cross section and the factor $\Gamma_{ab,N}$ contains all the collinear singularities (see, e.g., ref. [14]). This factor depends on the factorization (or regularization) scale μ and the factorization scheme, but it is universal (process independent). Moreover, it fulfils the Altarelli-Parisi evolution equations

$$\frac{\partial}{\partial \ln \mu^2} \Gamma_{ab,N} = \sum_c P_{ac,N}\Big(\alpha_{\rm S}\big(\mu^2\big)\Big)\Gamma_{cb,N}\,, \tag{A.4}$$

with the initial condition $\Gamma_{ab,N}(\mu^2 = 0) = \delta_{ab}$ and where $P_{ac,N}(\alpha_{\rm S})$ are the N-moments of the Altarelli-Parisi probabilities, whose power series expansion in $\alpha_{\rm S}$ can be computed at any perturbative order.

Note that the antisymmetric cross section $\sigma_{A,N}^a$ is an odd quantity under charge conjugation. Thus we have $\sigma_{A,N}^a = -\sigma_{A,N}^{\bar{a}}$ and, in particular, $\sigma_{A,N}^{q_f} = -\sigma_{A,N}^{\bar{q}_f}$ and $\sigma_{A,N}^g = 0$. Analogous relations are valid for $\hat{\sigma}_{A,N}^a$.

[8] Exactly analogous definitions hold for the symmetric cross section $d\sigma_{\rm S}^a/dx$ and its N-moments $\sigma_{{\rm S},N}^a$.

We can now consider in detail the massless limit of the b-quark antisymmetric cross section $\sigma_{\rm A}$, that is, the first moment $\sigma^{q_f}_{A,N=1}$. Since $\hat{\sigma}^a_{A,N}$ is C-odd, eq. (A.3) gives

$$\sigma^{q_f}_{A,N=1} = \sum_{f'} \hat{\sigma}^{q_{f'}}_{A,N=1} \Gamma_{f'f,N=1}\,, \tag{A.5}$$

where

$$\Gamma_{f'f,N=1} \equiv \Gamma_{q_{f'}q_f,N=1} - \Gamma_{\bar{q}_{f'}q_f,N=1}\,. \tag{A.6}$$

Using eq. (A.4) and the property $P_{ac}(\alpha_{\rm S}) = P_{\bar{a}\bar{c}}(\alpha_{\rm S})$, which follows from the charge-conjugation invariance of QCD, we obtain the following evolution equation for the singular collinear factor on the right-hand side of eq. (A.5)

$$\frac{\partial}{\partial \ln \mu^2}\Gamma_{f'f,N=1} = \sum_{f''} \Big[P_{q_{f'}q_{f''},N=1}\big(\alpha_{\rm S}(\mu^2)\big) - P_{\bar{q}_{f'}q_{f''},N=1}\big(\alpha_{\rm S}(\mu^2)\big)\Big]\,\Gamma_{f''f,N=1}\,, \tag{A.7}$$

Note that the combination of first moments of the Altarelli-Parisi probabilities on the right-hand side of eq. (A.7) vanishes up to $\mathcal{O}(\alpha_{\rm S}^2)$:

$$P_{q_{f'}q_{f''},N=1}\big(\alpha_{\rm S}(\mu^2)\big) - P_{\bar{q}_{f'}q_{f''},N=1}\big(\alpha_{\rm S}(\mu^2)\big) = \mathcal{O}\big(\alpha_{\rm S}^3\big)\,. \tag{A.8}$$

This result follows from fermion-number conservation and it can be explicitly checked by using the known LO and NLO expressions [14] of the Altarelli-Parisi probabilities. Equation (A.8) implies that $\Gamma_{f'f,N=1} = \delta_{f'f} + \mathcal{O}(\alpha_{\rm S}^3)$ and, thus, the massless-quark antisymmetric cross section $\sigma^{q_f}_{A,N=1}$ is free from collinear singularities up to NNLO accuracy:

$$\sigma^{q_f}_{A,N=1} = \hat{\sigma}^{q_f}_{A,N=1} + \mathcal{O}\big(\alpha_{\rm S}^3\big)\,. \tag{A.9}$$

To conclude our argument on the finiteness of $\sigma^{q_f}_{A,N=1}$, we have to discuss the effect of soft singularities. The QCD factorization theorem guarantees that the short-distance cross section $\hat{\sigma}^{q_f}_{A,N}$ is finite for any value of the moment index $N > 1$. The limit $N \to 1$ of eqs. (A.2) and (A.3) has to be dealt with with care because it is sensitive to possible soft singularities of the type $d\sigma^{q_f}_{\rm A}/dx \sim 1/x$ in the inclusive quark spectrum. These singularities can arise when q_f is produced by the fragmentation of a soft gluon. At $\mathcal{O}(\alpha_{\rm S})$ there are no such fragmentation subprocesses. At $\mathcal{O}(\alpha_{\rm S}^2)$, there is only the subprocess $g \to q_f\bar{q}_f$. In this $\mathcal{O}(\alpha_{\rm S}^2)$-subprocess, however, the pair $q_f\bar{q}_f$ is produced in a definite state of positive charge conjugation and, thus, it gives a vanishing contribution to the C-odd cross section $\sigma^{q_f}_{\rm A}$. It follows that up to $\mathcal{O}(\alpha_{\rm S}^2)$ the limit $N \to 1$ can be safely performed and the right-hand side of eq. (A.9) is finite.

The antisymmetric cross section $\sigma_{\rm A}$ is the integral of a single-particle (parton) inclusive distribution and thus, the finiteness of eq. (A.9) may appear surprising. However, this result is not accidental. The collinear safety of $\sigma^{q_f}_{A,N=1}$ follows from fermion-number conservation, i.e., eq. (A.8), and this is exactly the same equation that, up to $\mathcal{O}(\alpha_{\rm S}^2)$, guarantees the finiteness of the Adler, Gross-Llewellyn-Smith and unpolarized-Bjorken sums in Deep-Inelastic-Scattering.

B. Integrating the *E*-terms

In this appendix we give some details of the integration of the E-terms appearing in, for example, eq. (4.9).

We begin with the symmetric term $\int E_{\rm S}$, which is equal to the total contribution to $R_{\rm e^+e^-}$ from four-b final states. We label the quark (antiquark) momenta as $p_{1,2}(p_{3,4})$ and retain all mass terms. The integral is then analogous to eq. (B.2) of ref. [13], but with the massless phase space replaced by that with four equal final-state masses:

$$\int E_{\rm S} = \frac{1}{(2!)^2} C_{\rm F} \Big(\frac{\alpha_{\rm S}}{2\pi}\Big)^2 \frac{1}{Q^2} \int d\Phi_4\big(Q^2; m_b^2, m_b^2, m_b^2, m_b^2\big) \times \\ \times \Big[E_{\rm S}\big(p_1,p_2,p_3,p_4\big) + \big(p_1 \leftrightarrow p_2\big) + \big(p_3 \leftrightarrow p_4\big) + \big(p_1 \leftrightarrow p_2, p_3 \leftrightarrow p_4\big)\Big], \tag{B.1}$$

and with the E-term itself in eq. (B.7) of ref. [13] replaced by:

$$\begin{aligned} E_{\rm S} = \Big(C_{\rm F} - \frac{C_{\rm A}}{2}\Big)\Bigg\{\Bigg[\Bigg(\Big(&s_{12}s_{23}s_{34} - s_{12}s_{24}s_{34} + s_{12}s_{14}s_{34} + s_{12}s_{13}s_{34} + s_{13}s_{24}^2 - \\ &- s_{14}s_{23}s_{24} + s_{13}s_{23}s_{24} + s_{13}s_{14}s_{24} + s_{13}^2 s_{24} - s_{14}s_{23}^2 - s_{14}^2 s_{23} - s_{13}s_{14}s_{23}\Big) - \\ &- 2m_b^2\Big(2s_{12}s_{13} + 3s_{12}s_{14} + s_{12}s_{23} - s_{12}s_{24} - s_{12}s_{34} + 2s_{13}s_{14} + s_{13}s_{24} + \\ &+ s_{13}^2 + s_{14}s_{23} + s_{14}s_{24} + s_{14}s_{34} - s_{23}s_{24} - s_{23}s_{34} - s_{23}^2 - 3s_{24}s_{34} - s_{34}^2\Big) + \\ &+ 4m_b^4\Big(s_{12} + 2s_{13} + 5s_{14} + s_{23} - 2s_{24} - 3s_{34}\Big) - 16m_b^6\Big)\Big/\Big(s_{13}s_{23}s_{123}s_{134}\Big) - \\ &- \Big(s_{12}\Big(s_{12}s_{34} - s_{23}s_{24} - s_{13}s_{24} - s_{14}s_{23} - s_{14}s_{13}\Big) - 2m_b^2\Big(4s_{12}s_{34} + 2s_{12}^2 - \\ &- 2s_{13}s_{14} - 2s_{13}s_{23} - 2s_{13}s_{24} - s_{13}^2 - 2s_{14}s_{23} - 2s_{23}s_{24} - s_{23}^2\Big) - \\ &- 4m_b^4\Big(-6s_{12} + 2s_{13} + s_{14} + 2s_{23} + s_{24} - 3s_{34}\Big) - 24m_b^6\Big)\Big/\Big(s_{13}s_{23}s_{123}^2\Big) - \\ &- \Big(\Big(s_{14} + s_{13}\Big)\Big(s_{24} + s_{23}\Big)s_{34} - m_b^2\Big(2s_{12}s_{13} + 2s_{12}s_{23} + s_{12}s_{34} + s_{12}^2 + \\ &+ 4s_{13}s_{23} + s_{13}s_{24} + s_{13}s_{34} + s_{13}^2 + s_{14}s_{23} - s_{14}s_{34} + s_{23}s_{34} + s_{23}^2 - s_{24}s_{34}\Big) - \\ &- 2m_b^4\Big(-2s_{12} - s_{13} + 3s_{14} - s_{23} + 3s_{24} + 2s_{34}\Big) + 24m_b^6\Big)\Big/\Big(s_{13}s_{23}s_{134}s_{234}\Big)\Bigg] + \\ &+ \Big[\Big(p_1 \leftrightarrow p_3, p_2 \leftrightarrow p_4\Big)\Big]\Bigg\}, \end{aligned} \tag{B.2}$$

where $s_{ij} = (p_i + p_j)^2$ and $s_{ijk} = (p_i + p_j + p_k)^2 - m_b^2$. Note that by setting $m_b = 0$ we trivially recover the result of ref. [13].

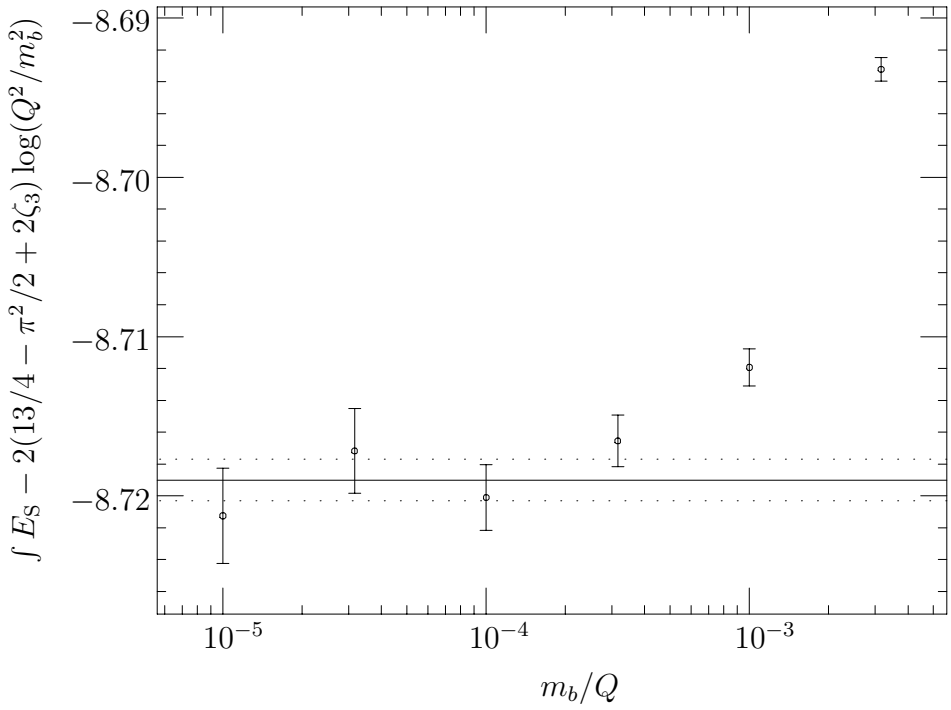

Figure 6: The term c in eq. (B.4) as a function of mass. The errors are purely from Monte Carlo statistics. The solid line is our fit to the limiting value and the dotted lines its error.

In the massless case, the integral is divergent in all four triple-collinear limits. When i, j and k are all collinear, we have $s_{ij} \sim s_{ik} \sim s_{jk} \sim s_{ijk} \to 0$ and the leading behaviour of the squared matrix element is $\sim 1/s_{ijk}^2$. Since the volume of three-body phase space is $\sim s_{ijk}$, we obtain a logarithmic divergence. Its coefficient is the integral of the corresponding Altarelli-Parisi splitting function (either $P_{q\bar{q}}^{NS}$ or $P_{\bar{q}q}^{NS}$, which are equal because of the charge-conjugation invariance of QCD). After summing over the four singular regions, we obtain one singular contribution for each of the two partons in the tree-level contribution, so we expect the coefficient of the logarithmically-enhanced term in eq. (B.1) to be

$$2\int_0^1 dz\, P_{q\bar{q}}^{NS}(z) = 2\left(\frac{13}{4} - \frac{\pi^2}{2} + 2\zeta_3\right). \tag{B.3}$$

That is, we expect the result retaining the quark mass to be of the form

$$\int E_{\rm S} = C_{\rm F}\left(C_{\rm F} - \frac{C_{\rm A}}{2}\right)\left(\frac{\alpha_{\rm S}}{2\pi}\right)^2\left[2\left(\frac{13}{4} - \frac{\pi^2}{2} + 2\zeta_3\right)\ln\frac{Q^2}{m_b^2} + c\right], \tag{B.4}$$

with c tending to a constant at small masses. Our numerical results confirm the coefficient of the log. For the constant term we obtain the results shown in figure 6. To obtain the limiting value, we have tried fitting various degree polynomials in m_b/Q to the points $m_b/Q \leq \mu_{\max}$, reducing $\mu_{\max}$ until the fit is acceptable. We call

the range of values from the different fits a systematic error, which is comparable to the statistical error, and add them in quadrature, to give:

$$c = -8.7190 \pm 0.0013. \tag{B.5}$$

At the Z peak, logs of the bottom quark mass are not yet asymptotic. Using the log-plus-constant approximation, we obtain

$$\int E_{\mathrm{S}} \left(\frac{m_b}{Q} = \frac{5}{91}\right) \approx C_{\mathrm{F}} \left(C_{\mathrm{F}} - \frac{C_{\mathrm{A}}}{2}\right) \left(\frac{\alpha_{\mathrm{S}}}{2\pi}\right)^2 \big[-0.3719 \pm 0.0015\big], \tag{B.6}$$

while direct integration gives

$$\int E_{\mathrm{S}} \left(\frac{m_b}{Q} = \frac{5}{91}\right) = C_{\mathrm{F}} \left(C_{\mathrm{F}} - \frac{C_{\mathrm{A}}}{2}\right) \left(\frac{\alpha_{\mathrm{S}}}{2\pi}\right)^2 \big[+0.8174 \pm 0.0001\big]. \tag{B.7}$$

Even so, the difference between the two results is still an order of magnitude smaller than $\alpha_{\mathrm{S}}^2 m_b/M_{\mathrm{Z}}$, the anticipated size of mass corrections.

For charm quarks however, the log-plus-constant approximation works quite well:

$$\int E_{\mathrm{S}} \left(\frac{m_c}{Q} = \frac{1.5}{91}\right) \approx C_{\mathrm{F}} \left(C_{\mathrm{F}} - \frac{C_{\mathrm{A}}}{2}\right) \left(\frac{\alpha_{\mathrm{S}}}{2\pi}\right)^2 \big[3.0922 \pm 0.0015\big], \tag{B.8}$$

$$\int E_{\mathrm{S}} \left(\frac{m_c}{Q} = \frac{1.5}{91}\right) = C_{\mathrm{F}}(C_{\mathrm{F}} - C_{\mathrm{A}}/2) \left(\frac{\alpha_{\mathrm{S}}}{2\pi}\right)^2 \big[3.3527 \pm 0.0003\big]. \tag{B.9}$$

We turn now to the integral $(2\int E_{\mathrm{A}} - \int E_{\mathrm{S}})$, which we claim is finite in massless QCD. If it is defined in the most natural way, eq. (B.10), the integrand is not piecewise finite, making it unsuitable for numerical integration. However, we can rewrite it in a form in which it is, proving the finiteness of the whole integral, and allowing it to be performed numerically.

If we define $E_{\mathrm{A}}(n)$ to be the E-term contribution that is antisymmetric with respect to the direction n, then our integral for the quark axis definition is

$$\int \Big(E_{\mathrm{A}}(p_1) + E_{\mathrm{A}}(p_2) - E_{\mathrm{S}}\Big)\,. \tag{B.10}$$

In each of the four triple-collinear limits $s_{ijk} \to 0$, the integrand diverges like $1/s_{ijk}^2$, again yielding a logarithmic divergence. The coefficient of this divergence is either positive or negative, depending on whether the collinear partons ijk are $qq\bar{q}$ or $q\bar{q}\bar{q}$.

However, using the fact that E_{A} is C-odd, we have the relation

$$\int E_{\mathrm{A}}(p_1) = \int E_{\mathrm{A}}(p_2) = -\int E_{\mathrm{A}}(p_3) = -\int E_{\mathrm{A}}(p_4)\,, \tag{B.11}$$

which we can exploit to rewrite eq. (B.10) as

$$\int \left(\frac{1}{2}E_{\mathrm{A}}(p_1) + \frac{1}{2}E_{\mathrm{A}}(p_2) - \frac{1}{2}E_{\mathrm{A}}(p_3) - \frac{1}{2}E_{\mathrm{A}}(p_4) - E_{\mathrm{S}}\right). \tag{B.12}$$

In each of the four collinear limits, two of the E_{A} terms have equal and opposite divergences to each other and two of them have equal and opposite divergences to E_{S}, yielding an integrable integrand with a finite result. We have thus proved that eq. (B.10) is finite.

Although this argument was formulated in terms of the b-quark axis definition, it applies equally well to any infrared-safe definition, like the thrust axis, since they must become equal in the triple-collinear limit.

Since the integrand is everywhere integrable, we can use the same numerical program as for the rest of the non-singlet contributions, and obtain the results in eqs. (4.10) and (4.11).

References

[1] The LEP collaborations ALEPH, DELPHI, L3, OPAL, the LEP Electroweak Working Group, and the SLD Heavy Flavour Group, *A Combination of Preliminary Electroweak Measurements and Constraints on the Standard Model*, report CERN-EP/99-15, February 1999.

[2] K. Mönig, *Running TESLA on the Z Pole*, talk given at the Worldwide Study on Physics and Experiments with Future Linear $\mathrm{e^+e^-}$ Colliders, Sitges, Spain, April 28-May 5, 1999, available from http://www.cern.ch/Physics/LCWS99/talks.html.

[3] J. Jersák, E. Laermann and P.M. Zerwas, *QCD corrected forward backward asymmetry of quark jets in* $\mathrm{e^+e^-}$ *annihilation*, *Phys. Lett.* **B 98** (1981) 363; *Electroweak production of heavy quarks in* $\mathrm{e^+e^-}$ *annihilation*, *Phys. Rev.* **D 25** (1982) 1218, erratum *Phys. Rev.* **D 36** (1987) 310.

[4] A.B. Arbuzov, D.Yu. Bardin and A. Leike, *Analytic final state corrections with cut for* $\mathrm{e^+e^-} \to$ *massive fermions*, *Mod. Phys. Lett.* **A 7** (1992) 2029, erratum *Mod. Phys. Lett.* **A 9** (1994) 1515.

[5] A. Djouadi, B. Lampe and P.M. Zerwas, *A note on the QCD corrections to forward-backward asymmetries of heavy Quark jets in Z decays*, *Z. Physik* **C 67** (1995) 123 [hep-ph/9411386].

[6] B. Lampe, *A note on QCD corrections to* A_{FB}^b *using thrust to determine the b-quark direction*, hep-ph/9812492.

[7] G. Altarelli and B. Lampe, *Second order QCD corrections to heavy quark forward-backward asymmetries*, *Nucl. Phys.* **B 391** (1993) 3.

[8] V. Ravindran and W.L. van Neerven, *Second order QCD corrections to the forward-backward asymmetry in* $\mathrm{e^+e^-}$ *collisions*, *Phys. Lett.* **B 445** (1998) 214 [hep-ph/9809411].

JHEP07(1999)023

[9] A. Blondel, B.W. Lynn, F.M. Renard and C. Verzegnassi, *Precision measurements of final state weak coupling from polarized electron-positron annihilation*, *Nucl. Phys.* **B 304** (1988) 438.

[10] A.H. Hoang, M. Jeżabek, J.H. Kühn and T. Teubner, *Radiation of heavy quarks*, *Phys. Lett.* **B 338** (1994) 330 [hep-ph/9407338].

[11] M.H. Seymour, *Heavy quark pair multiplicity in* e^+e^- *events*, *Nucl. Phys.* **B 436** (1995) 163.

[12] D. Abbaneo et al., *QCD corrections to the forward-backward asymmetries of c and b quarks at the Z pole*, *Eur. Phys. J.* **C 4** (1998) 185.

[13] R.K. Ellis, D.A. Ross and A.E. Terrano, *The perturbative calculation of jet structure in* e^+e^- *annihilation*, *Nucl. Phys.* **B 178** (1981) 421.

[14] G. Curci, W. Furmanski and R. Petronzio, *Evolution of parton densities beyond leading order: the non-singlet case*, *Nucl. Phys.* **B 175** (1980) 27;
G. Altarelli, *Partons in quantum chromodynamics*, *Phys. Rep.* **81** (1982) 1; and references therein.

[15] K.G. Chetyrkin, A.L. Kataev and F.V. Tkachov, *Higher order corrections to* σ_T *(*$e^+e^- \to$ *hadrons) in quantum chromodynamics*, *Phys. Lett.* **B 85** (1979) 277;
W. Celmaster and R.J. Gonsalves, *An analytic calculation of higher order quantum chromodynamic corrections in* e^+e^- *annihilation*, *Phys. Rev. Lett.* **44** (1980) 560.

[16] P.J. Rijken and W.L. van Neerven, *Higher order QCD corrections to the transverse and longitudinal fragmentation functions in electron-positron annihilation*, *Nucl. Phys.* **B 487** (1997) 233 [hep-ph/9609377]; $O(\alpha_S^2)$ *contributions to the longitudinal fragmentation function in* e^+e^- *annihilation*, *Phys. Lett.* **B 386** (1996) 422 [hep-ph/9604436].

[17] S. Catani and M.H. Seymour, *The dipole formalism for the calculation of QCD jet cross-sections at next-to-leading order*, *Phys. Lett.* **B 378** (1996) 287 [hep-ph/9602277]; *A general algorithm for calculating jet cross-sections in NLO QCD*, *Nucl. Phys.* **B 485** (1997) 291 [hep-ph/9605323], erratum *Nucl. Phys.* **B 510** (1997) 503.

[18] E.B. Zijlstra and W.L. van Neerven, *Order* α_S^2 *QCD corrections to the deep inelastic proton structure functions* F_2 *and* F_L, *Nucl. Phys.* **B 383** (1992) 525.

[19] W.T. Giele and E.W.N. Glover, *Higher order corrections to jet cross-sections in* e^+e^- *annihilation*, *Phys. Rev.* **D 46** (1992) 1980.

[20] P.J. Rijken and W.L. van Neerven, $O(\alpha_S^2)$ *contributions to the asymmetric fragmentation function in* e^+e^- *annihilation*, *Phys. Lett.* **B 392** (1997) 207 [hep-ph/9609379].

JHEP07(1999)023